BMC Medical Imaging

RESEARCH

Open Access

Study on heterogeneity of vascularity and cellularity via multiparametric MRI habitat imaging in breast cancer

Xiaolei Zhang[1†], Xiaoyan Chen[1†], Yao Fu[1], Han Zhou[1] and Yan Lin[1*]

Abstract

Background This study aimed to visually analyze the heterogeneity of vascularity and cellularity across different sub-regions of breast cancer using habitat imaging (HI) to predict human epidermal growth factor receptor 2 (HER2) expression and evaluate the effectiveness of neoadjuvant therapy (NAT) in breast cancer patients.

Methods A retrospective analysis was conducted on 76 patients diagnosed with breast cancer. Diffusion-weighted imaging (DWI) and dynamic contrast-enhanced MRI (DCE-MRI) sequences were utilized to acquire MR images. Apparent diffusion coefficient (ADC), K^{trans}, K_{ep}, and V_e values were measured for each sub-region, and the percentage of each sub-region relative to the total lesion was calculated. Statistical analyses, including t-tests, rank-sum tests, chi-square tests, and Spearman correlation, were performed.

Results Three distinct sub-regions within breast cancer lesions were identified through HI, characterized physiologically as: low vascularity–high cellularity (LV-HC), low vascularity–low cellularity (LV-LC), and high vascularity–low cellularity (HV-LC). Significant differences were observed in the proportions of these tumor sub-regions between HER2-positive and HER2-negative breast cancers. Additionally, HER2-low and HER2-zero breast cancers demonstrated statistical differences in the second sub-region (LV-LC). Furthermore, the proportion of the first sub-region (LV-HC) was negatively correlated with the efficacy of NAT in breast cancer patients.

Conclusions Habitat imaging can identify distinct sub-regions within breast cancer lesions, providing a noninvasive imaging biomarker for predicting HER2 expression levels and assessing the efficacy of NAT in breast cancer patients.

Keywords Breast cancer, Tumor heterogeneity, Habitat imaging, Multiparametric MRI, HER2 expression

†Xiaolei Zhang and Xiaoyan Chen contributed equally to this work.

*Correspondence:
Yan Lin
994809889@qq.com
[1]Department of Radiology, Second Affiliated Hospital of Shantou University Medical College, No. 69, Dongxiabei Road, Jinping District, Shantou, Guangdong Province 515041, China

Introduction

Breast cancer is not only the most prevalent malignancy worldwide, but also the leading cause of cancer-related death in women [1]. In fact, personalized medicine is crucial for improving the clinical outcomes of breast cancer patients [2–4]. However, the high degree of inter-tumor and intra-tumor heterogeneity of breast cancer poses a major obstacle to the clinical implementation of individualized treatment [5, 6].

Inter-tumor heterogeneity refers to the existence of heterogeneity among tumors of the same histological type, so breast cancer can be classified into different molecular types by immunohistochemistry (IHC) and fluorescence in situ hybridization (FISH) [7]. The first principle of molecular typing is to interpret the status of human epidermal growth factor receptor 2 (HER2), which is closely related to tumor angiogenesis and tumor cell proliferation [8]. In brief, HER2 is an important molecular marker in breast cancer. Based on the amplification of the HER2 gene and the level of HER2 protein expression, breast cancer is classified into HER2-positive and HER2-negative types. HER2-negative breast cancer is further divided into two groups: HER2-low and HER2-zero [9, 10]. The specific definitions are as follows: HER2-positive: Defined as IHC 3 + or IHC 2+/FISH+; HER2-low: Defined as IHC 1 + or IHC 2 + with FISH-; HER2-zero: Defined as IHC 0.

Breast cancer with different HER2 expression levels shows heterogeneity in vascularity and cellularity [11, 12]. Traditionally, breast cancer was classified into HER2-positive and HER2-negative based on the HER2 gene and its receptor. In recent years, the development of anti-HER2 antibody-drug conjugates has led to clinical trials that have unveiled the potential benefits of treating HER2-low breast cancer and derived a novel clinical therapeutic phenotype [13]. The heterogeneity within breast cancer tumors also poses significant challenges to individualized treatment, affecting patient's response to neoadjuvant therapy (NAT) [14, 15]. Breast cancer is a complex ecosystem as it harbors variations in angiogenesis and tumor cell abundance in different regions under microenvironmental selection pressures. Particularly, inadequate local oxygen supply to the tumor can lead to the formation of a hypoxic environment that increases the tolerance of tumor cells to therapeutic drugs [16]. Therefore, the evaluation of vascularity and cellularity heterogeneity in inter- and intra-tumor regions of breast cancer is beneficial for predicting the HER2 expression levels and assessing the effectiveness of NAT, further to promote the development of personalized medicine.

Pathological diagnosis is the gold standard for assessing tumor heterogeneity [17, 18], but its invasiveness, sampling limitations and sample dependence make it incapable of adequately characterizing tumor heterogeneity. Magnetic resonance imaging (MRI) has the characteristics of multi-direction, multi-parameter, high soft-tissue resolution and non-radiation, which can provide comprehensive diagnostic information on morphology, functionality, metabolism, and hemodynamics [19, 20]. In addition, habitat imaging (HI) achieved by clustering similar voxels in the multi-parameter images can fully and completely depict the biological characteristics of different regions within the tumor [21–24], allowing the tumor to be divided into different sub-regions. This suggests that if these techniques are implemented in a clinical setting, they have the potential to enhance clinicians' assessment of heterogeneity within breast cancer tumors, thereby providing valuable insights into patients' treatment sensitivity.

In current clinical practice, the evaluation of HER2 status relies on invasive histopathological techniques such as immunohistochemistry (IHC) and fluorescence in situ hybridization (FISH). These methods are limited by sampling bias and insufficient spatial representation, which may fail to capture the full extent of intra-tumor heterogeneity and potentially lead to HER2 misclassification, thereby affecting treatment decisions. Moreover, in breast cancer patients undergoing neoadjuvant therapy (NAT), there is a lack of sensitive, accurate, and reproducible imaging methods to predict treatment efficacy at an early stage. Traditional assessments based on tumor size changes are often delayed and may result in missed opportunities for timely treatment adjustment.

Given these limitations, MRI—particularly HI derived from multiparametric MRI—offers a promising non-invasive approach for characterizing tumor heterogeneity in terms of vascularity and cellularity. HI has the potential to serve as an imaging biomarker for predicting HER2 expression and evaluating NAT response, thereby addressing key gaps in current clinical workflows and contributing to the advancement of personalized breast cancer management.

Hence, this study aimed to use multi-parameter MRI and HI to visually analyze the heterogeneity of vascularity and cellularity in different habitat subregions of breast cancer, so as to predict the expression level of HER2 and the efficacy of NAT in breast cancer patients.

Methods

Study population

This retrospective study has been approved by the Institutional Review Board. Seventy-six patients were recruited from the Second Affiliated Hospital of Shantou University Medical College (official website: https://www.st120.cn/) between January 2017 and November 2022. Patient characteristics were summarized in Table 1. Inclusion and exclusion criteria were shown in Fig. 1. A

Table 1 Summary of demographic and clinical data from the study cohorts

Parameter	the Study Cohorts($n=76$)
Age	
Median*	51(33–74)
Estrogen receptor	
Positive	50(66)
Negative	26(34)
Progesterone receptor	
Positive	38(50)
Negative	38(50)
Human epidermal growth factor receptor type 2	
Positive	24(32)
Negative	52(68)
Low	33(63)
Zero	19(37)
Histologic	
Invasive ductal carcinoma	61(80)
Invasive lobular carcinoma	4(5)
Other	11(15)
Pathologic grade	
1	4(5)
2	41(54)
3	24(32)
Unknown	7(9)
Lymph node metastasis	
Yes	41(54)
No	29(38)
Unknown	6(8)

Note. Unless otherwise indicated, data are numbers of patients, with percentages in parentheses

*Numbers in parentheses are the range

brief description of the inclusion and exclusion criteria was provided as follows.

Inclusion criteria: (1) High-risk populations undergoing breast MRI screening; (2) Suspected breast lesions detected through clinical palpation, mammography, and breast ultrasound; (3) No prior surgery, chemotherapy, endocrine therapy, radiotherapy, or other anti-tumor treatments before breast MRI examination.

Exclusion criteria: (1) Poor image quality due to motion artifacts; (2) MRI dynamic contrast-enhanced examination not performed due to contrast agent allergy; (3) Lack of pathological histology results; (4) Pathological confirmation of benign lesions after MRI; (5) Incomplete immunohistochemistry results; (6) MRI-related contraindications.

MR acquisition

In this study, patients were imaged using a 3.0 T scanner (GE Medical System, Milwaukee, WI, USA) with a dedicated four-channel bilateral breast coil. The protocol parameters of diffusion weighted image (DWI) and dynamic contrast enhanced-MRI (DCE-MRI) were listed in Table 2. In detail, we utilized a 3.0T superconducting MRI scanner from GE Medical System (Milwaukee, WI, USA) along with a dedicated four-channel bilateral breast coil to collect all MRI data. During the examination, all patients were positioned in the prone position with both breasts naturally suspended within the breast coil, ensuring the chest wall was in close contact with the coil to avoid skin folds around the periphery. The scanning sequences included DWI and DCE-MRI. For DCE-MRI, the VIBRANT sequence was used, with 64-phase scanning settings. After five initial pre-scans, gadolinium-based contrast agent (Gadoleric Acid Meglumine Salt Injection, Jiangsu, China) was intravenously injected using a high-pressure injector at a flow rate of 2 ml/s and a dosage of 0.2 ml/kg, with continuous scanning during the remaining phases. DWI was performed using the postprocess software Functool 9 of GE MR imager, yielding apparent diffusion coefficient (ADC) maps. Based on the standard map and the improved Tofts model, the function diagrams of volume transfer constant (K^{trans}), flux rate constant (K_{ep}) and extracellular volume fraction (V_e) of the whole breast lesion were obtained.

In practice, DCE sequences can calculate and analyze quantitative parameters such as the K^{trans}, K_{ep}, and V_e using the two-compartment Tofts model. K^{trans} reflects the rate at which the contrast agent moves from the vascular space into the extravascular extracellular space, K_{ep} reflects the rate at which the contrast agent moves back from the extravascular extracellular space to the plasma, and V_e reflects the fraction of the total volume occupied by the extravascular-extracellular tissue space in the unit volume.

In this study, we employed DWI and DCE-MRI to assess tumor vascularity and cellularity. However, these imaging techniques do have certain technical limitations. First, although we minimized motion artifacts using respiratory training and fast imaging sequences, slight patient movement may still affect image quality. To minimize the impact of motion artifacts on our results, we conducted strict quality control of all images and excluded any data with significant motion artifacts or poor image quality. Second, partial volume effects could affect the ADC values of small lesions (diameter < 1 cm), potentially leading to underestimation of their true values. In our data analysis, we excluded these small lesions to ensure that the tumors selected for analysis were of sufficient size to minimize the impact of partial volume effects.

Image analysis and segmentation

All data analysis and segmentation were independently conducted by three experienced radiologists. Using 3D-slicer 5.0.3 software, tumor regions-of-interest (ROI)

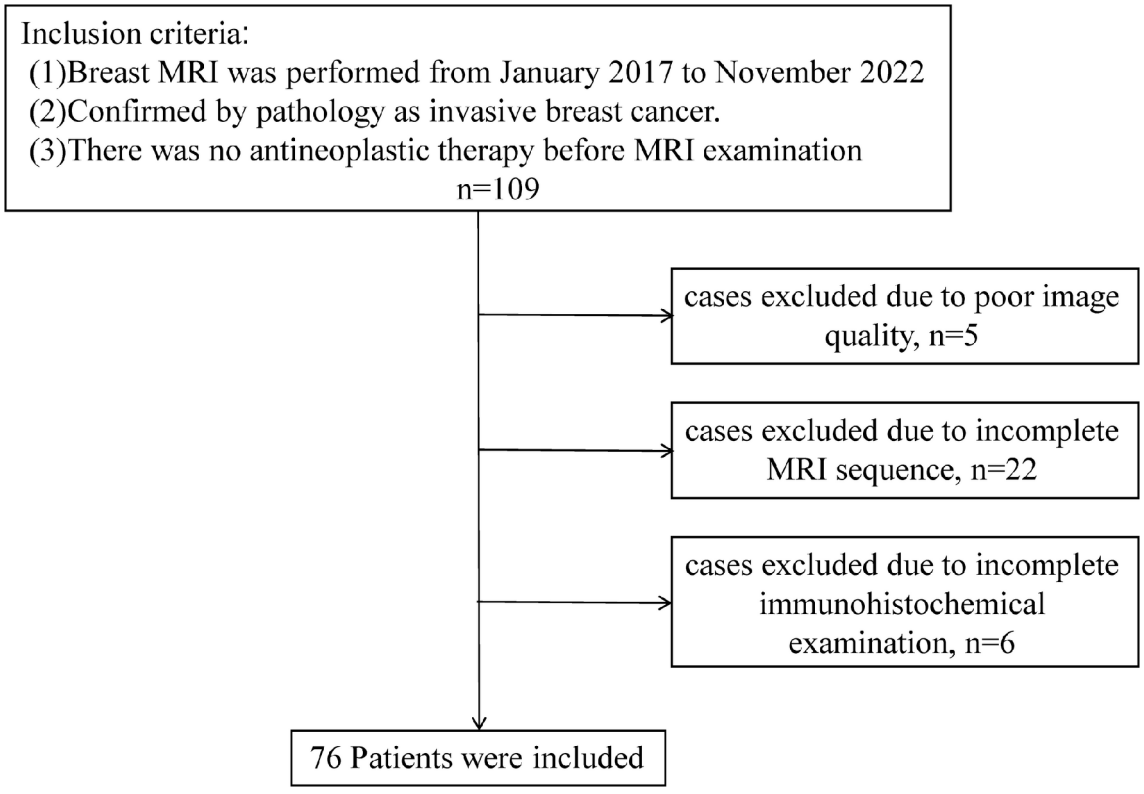

Fig. 1 Flowchart of the study population

Table 2 Imaging parameters for DWI and DCE-MRI

Parameter	DWI	DCE-MRI
Sequence	DW-EPI	VIBRANT
Repetition time (ms)	5000	3.9
Echo time (ms)	91	2.1
Field of view (cm)	35	35
Fat suppression	STIR	SPECIAL
Matrix	128×128	256×256
Bandwidth (Hz/pixel)	250	83.3
b values (s/mm^2)	0, 800	-
b direction	3	
Number of diffusion directions	3	-
Total scan time (s)	200	326

EPI = Echo Planar Imaging; VIBRANT = Volume Imaging for Breast Assessment; STIR = Short inversion-Time Inversion Recovery; SPECIAL = Spectral Inversion at Lipids

were manually delineated around the tumor boundary for all slices that contain the tumor based on the last phase of DCE to generate volume of interest (VOI). The VOI was manually registered with ADC, K^{trans}, K_{ep} and V_e maps. In detail, the DICOM files of the DWI sequence, DCE sequence, and the corresponding ADC, K^{trans}, K_{ep}, and V_e pseudocolor maps derived from them for all enrolled patients were imported into 3D-Slicer software. First, the ROI of the breast cancer lesions was manually delineated slice by slice on the last phase of the DCE-MRI sequence to form the VOI. Finally, using the last phase of the DCE-MRI sequence as the reference, the manually delineated VOI was registered with the ADC, K^{trans}, K_{ep}, and V_e pseudocolor maps. Image analysis and segmentation were shown in Fig. 2.

Discovery of tumor habitat

In this study, the fuzzy c-means (FCM) [25–28] that implemented in MATLAB software (https://www.mathworks.com/help/fuzzy/fuzzy-clustering.html) was used to cluster all lesions VOIs based on the voxel matrix established by ADC, K^{trans}, K_{ep} and V_e maps, and the flow chart of the method below was shown in Fig. 3. The flow chart of FCM clustering was displayed in Supplementary Information FILE S1.

The registered images were resampled to obtain isotropic voxel sizes, the final voxel size obtained was 1 mm × 1 mm × 1 mm. The multi-parametric voxel data of each lesion VOI was organized into a four-dimensional vector (ADC, K^{trans}, K_{ep}, V_e) for each voxel. The FCM algorithm was employed to conduct cluster analysis on the multi-parametric MRI images, assigning each pixel to its respective cluster. This division allowed for identifying different tumor habitat within the lesion, which were then visualized on the last phase image of the DCE sequence. To evaluate vascularity and cellularity, the average value of the multi-parametric quantitative

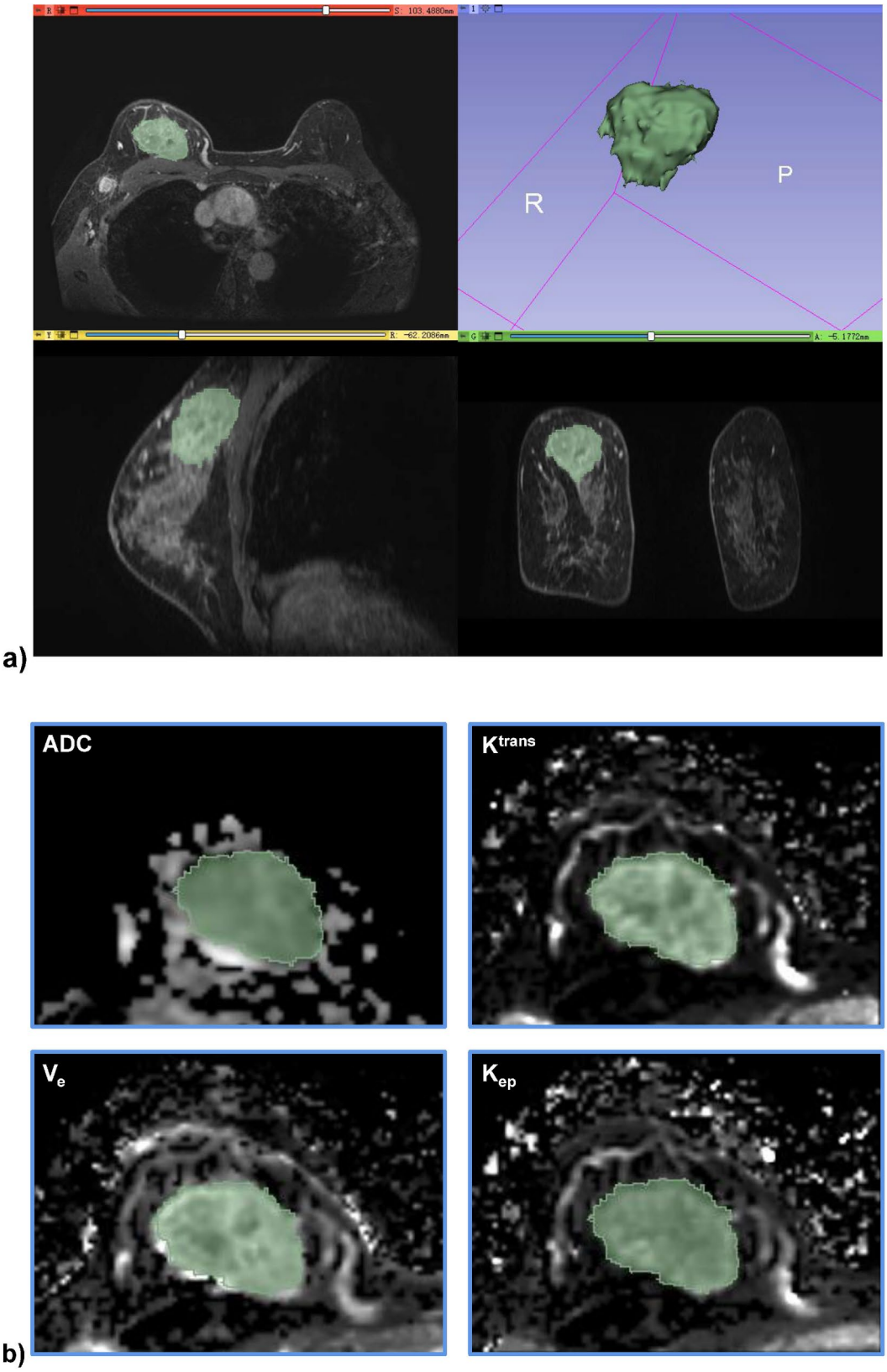

Fig. 2 Image analysis and segmentation. **a** A 3D-slicer sketch map of the breast cancer focus VOI. **b** a multi-parameter MRI image registration map

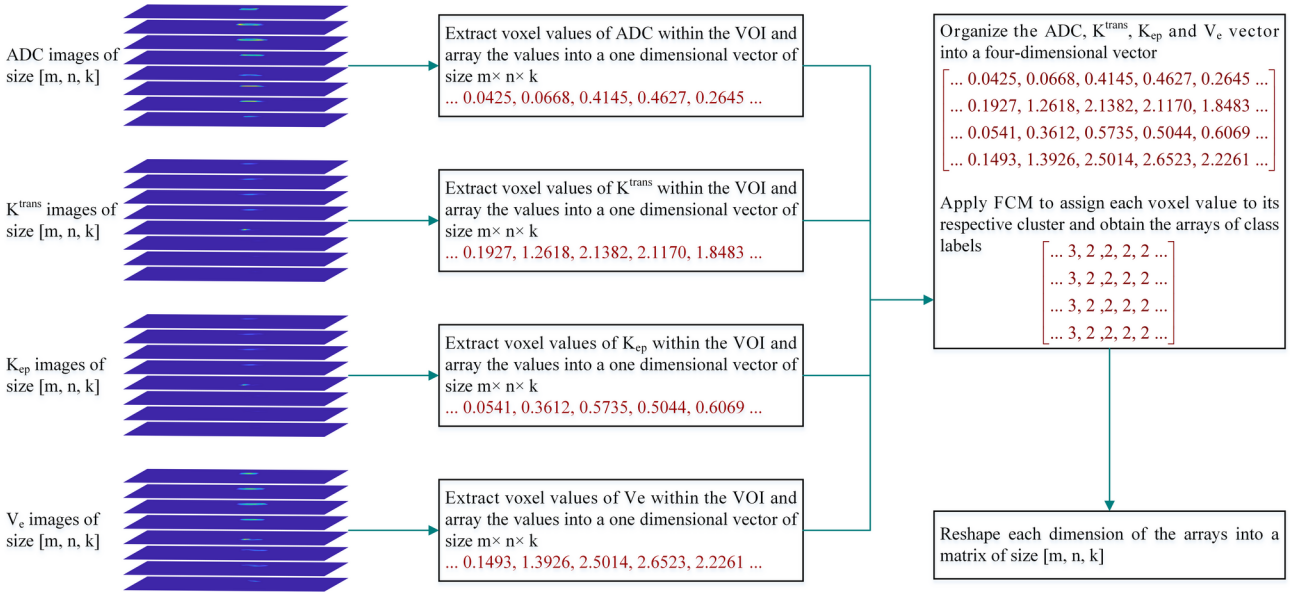

Fig. 3 Flowchart of FCM based lesions VOIs clustering

indicators was measured in each sub-region. Additionally, the percentage of each sub-region in each total lesion was determined.

To assess the vascularity and cellularity within each sub-region, we employed the mean values of K^{trans} and K_{ep} to evaluate vascularity, and used the mean values of ADC and V_e to assess cellularity. To examine the heterogeneity of intratumoral vascularity and cellularity, we measured the mean values of four quantitative indicators (K^{trans}, K_{ep}, ADC, and V_e) in three spatial habitat sub-regions, i.e., LV-HC (low blood flow perfusion, high cellular density), LV-LC (low blood flow perfusion, low cellular density), and HV-LC (high blood flow perfusion, low cellular density). Higher K^{trans} and K_{ep} values indicate better blood flow perfusion, while lower V_e and ADC values suggest higher cellular density. We established thresholds for these parameters to classify the study regions into three distinct sub-regions. The thresholds were chosen based on preclinical studies and the biological characteristics of tumor tissues, aiming to define the heterogeneity of different regions in terms of blood perfusion and cellular proliferation.

Pathology and immunohistochemistry

Two pathologists independently analyzed the pathology and immunohistochemistry of breast lesions and reached a consensus. All invasive breast cancer lesions were tested for the expression of estrogen receptor (ER), progesterone receptor (PR), C-erBb-2, and Ki-67. The expression of ER and PR was defined as nuclear positive staining ≥ 1% in 10 high-power fields. The result of HER2-positive is defined as the immunohistochemical result of C-erBb-2 (+++) or the gene amplification observed by FISH. Lesions with C-erBb-2 (++) were further tested using FISH.

In addition, the Miller&Payne (MP) evaluation system was used to evaluate the cell richness of residual invasive tumors in the primary breast after neoadjuvant therapy, which was divided into five grades. Specifically, the MP grading system includes the following five levels [29]:

- Grade 1 (G1): No change in infiltrating cancer cells or only a few cancer cells are altered, with no overall reduction in the number of cancer cells.
- Grade 2 (G2): Infiltrating cancer cells are mildly reduced, but their overall number remains high, with a decrease of no more than 30%.
- Grade 3 (G3): Infiltrating cancer cells are reduced by 30–90%.
- Grade 4 (G4): Infiltrating cancer cells are significantly reduced by more than 90%, with only small clusters or single cancer cells remaining.
- Grade 5 (G5): No infiltrating cancer cells are present at the original tumor bed, although ductal carcinoma in situ may still be present.

Statistical analysis

Prior to hypothesis testing, the Shapiro–Wilk test was applied to assess the normality of continuous variables. Variables with a normal distribution were analyzed using independent-samples t-tests, while non-normally distributed variables were assessed using the Mann–Whitney U test. Categorical variables were compared using chi-square tests. The relationship between the proportion of each spatial sub-region and the efficacy of neoadjuvant

therapy (Miller–Payne grading) was evaluated using Spearman's rank correlation.

As our study focused on three pre-defined tumor sub-regions with clear physiological interpretations, multiple comparisons corrections (e.g., Bonferroni or FDR) were not applied to avoid over-adjustment and potential Type II errors. Nevertheless, we acknowledge the implications of multiple testing and have added clarification regarding this aspect. All statistical analyses were conducted using SPSS Statistics 26.0 [30, 31]. Two-tailed p-values less than 0.05 were considered statistically significant.

Results

Clinical-Pathologic findings

This study included 76 patients with breast cancer, including 24 HER2-positive patients and 52 HER2-negative patients. For HER2-negative lesions, 33 cases had low expression of HER2 (HER2-low) and 19 had no expression of HER2 (HER2-zero). In these 76 patients, 23 received full-course of neoadjuvant therapy. Figure 4 displayed the multi-parametric MRI images of breast cancer patients with varying levels of HER2 expression.

Identification of tumor habitat in breast cancer

In this study, breast cancer tumors were physiologically divided into three sub-regions, including relatively low vascularity - high cellularity (LV - HC) region, relatively low vascularity - low cellularity (LV - LC) region, and relatively high vascularity - low cellularity (HV - LC) region. All breast cancer lesions of this cohort were divided into three spatial habitat sub-regions, as illustrated in Fig. 5.

In the evaluation of vascularity, we observed that the average value of K^{trans} was 1.032 (min^{-1}) and the average value of K_{ep} was 1.179 (min^{-1}) in the third sub-region, thus categorizing it as "relatively high vascularity". In contrast, the average values of K^{trans} in the first and second sub-regions were 0.099 (min^{-1}) and 0.141 (min^{-1}) respectively, and the average values of K_{ep} were 0.319 (min^{-1}) and 0.362 (min^{-1}) respectively, thus indicating that they behaved "relatively low vascularity". Regarding cellularity assessment, the average value of ADC in the first sub-region was $0.176 \times 10^{-3} mm^2/s$ and the average value of V_e was 0.196, which were labeled as "relatively high cellularity". On the other hand, the average values of ADC in the second and third sub-regions were $1.609 \times 10^{-3} mm^2/s$ and $1.094 \times 10^{-3} mm^2/s$ respectively, and the average values of V_e were 0.318 and 0.688 respectively, indicating that they were labeled as "relatively low cellularity" (see Table 3).

The volume proportion of each sub-region in breast cancer lesions with different HER2 expression levels

To quantify tumor heterogeneity in breast cancer with varying HER2 expression levels, we first measured the proportion of volume of each sub-region. Subsequently, we compared these proportions in breast cancers with different HER2 expression levels. Mann-Whitney U test analysis revealed a statistically significant difference between HER2-positive and HER2-negative breast cancer patients for the proportion of the volume in three sub-regions. The volume proportion of HER2-positive cases in the first sub-region was lower than that of HER2-negative cases, while the volume proportion of HER2-positive cases in the second and third sub-regions was higher than that of HER2-negative cases (p-value less than 0.05), as shown in Table 4. Similarly, the volume proportion of the second sub-region was lower in the HER2-low group compared to the HER2-zero group (p-value less than 0.05). However, there were no statistically significant difference between the HER2-low group and the HER2-zero group in the volume proportion of the first and third sub-regions (Table 5).

Correlation analysis between the proportion of each Spatial habitats and the efficacy of neoadjuvant therapy

The proportion of the first spatial sub-region (LV-HC) was negatively correlated with MP grading (Supplementary Information FIGURE S1). This suggested that the lower the proportion of the first spatial sub-region in breast cancer lesions, the better the efficacy of neoadjuvant therapy in patients (p-value less than 0.05).

Discussion

Breast cancer displays a high degree of heterogeneity, which can influence patients' response to treatment and ultimately affect their clinical outcomes [32]. Therefore, it is crucial to monitor and quantify tumor heterogeneity during diagnosis and treatment of breast cancer. The aim of this study was to visually analyze the heterogeneity of vascularity and cellularity of breast cancer by using multi-parameter MRI and HI.

Our findings showed that HI can be used to quantify the heterogeneity of vascularity and cellularity within and between breast cancers. We further observed that these three subregions had statistically significant differences between patients with HER2-positive and HER2-negative breast cancer, and HER2-low and HER2-zero breast cancer were statistically different in the second sub-region (relatively LV - LC). Furthermore, the ratio of subregion 1 (relatively LV-HC) was inversely associated with NAT response. These findings suggest that HI has the capability to quantify the heterogeneity of vascularity and cellularity in breast cancers with varying HER2 expression levels. So HI has the potential to serve as a non-invasive imaging predictor of neoadjuvant therapy efficacy in breast cancer.

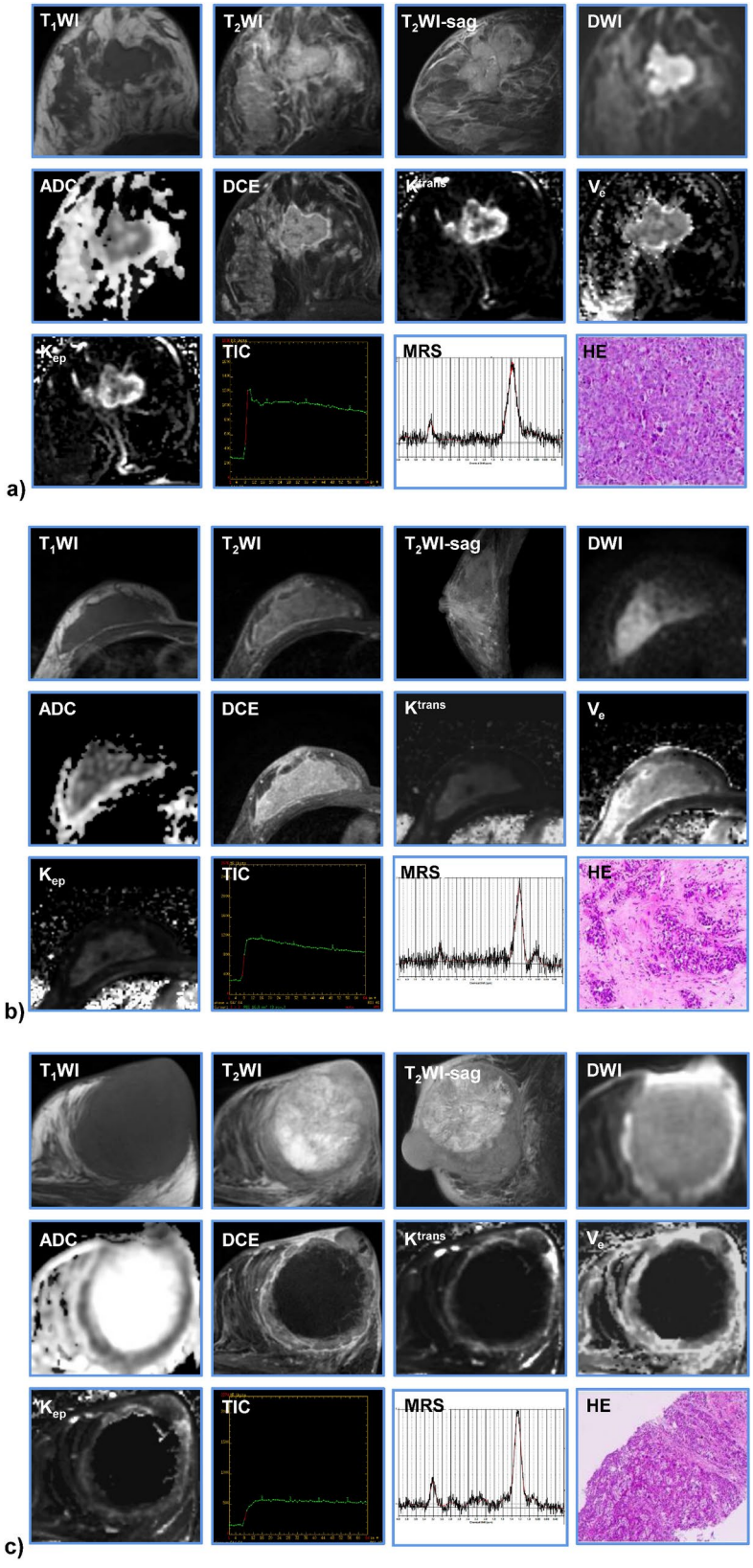

Fig. 4 Three cases of breast cancer lesions. **a** Invasive ductal breast carcinoma (IHC 2+ with an amplified FISH assay). **b** Invasive ductal breast carcinoma (IHC 2+ with a non-amplified FISH assay). **c** Invasive ductal breast carcinoma (IHC 0)

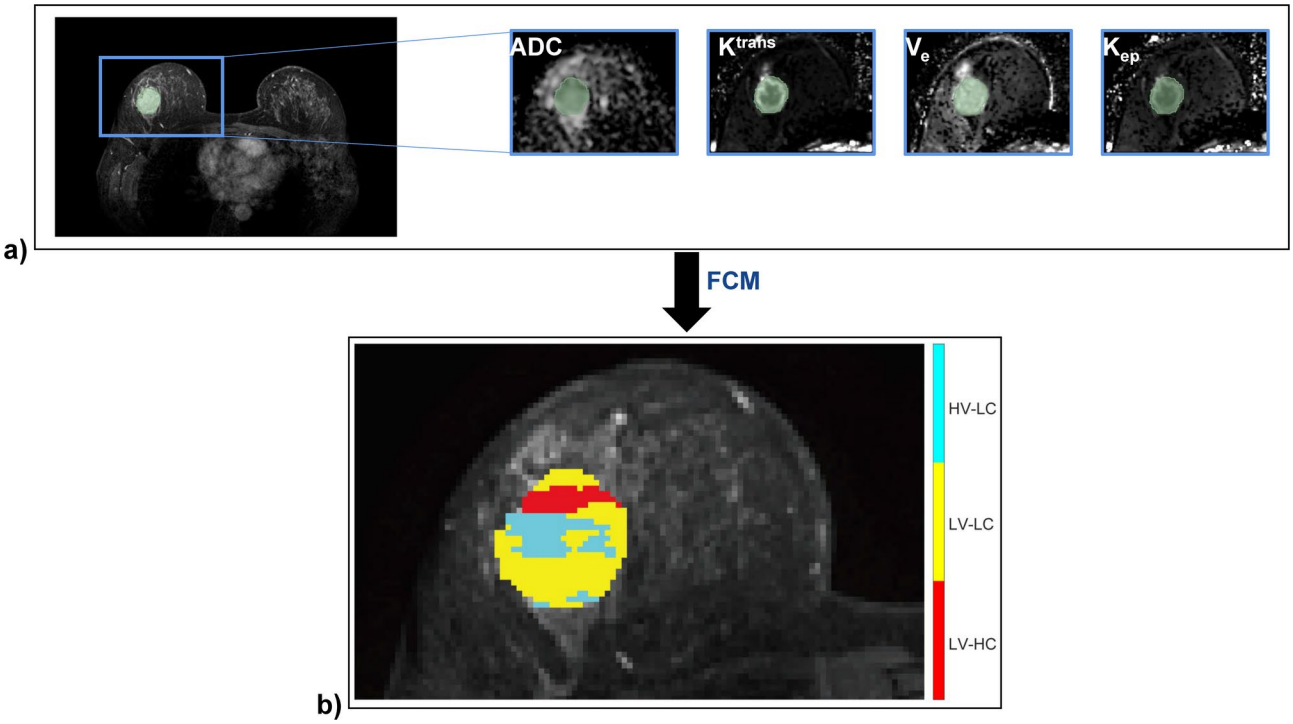

Fig. 5 An example of three divided spatial habitat sub-regions. **a** VOI of breast cancer lesions was sketched and aligned with quantitative parameter maps of ADC, k^{trans}, V_e and K_{ep}. **b** FCM clustering algorithm was used to identify different habitat sub-regions of breast lesions

Table 3 Average values of ADC, K^{trans}, V_e, K_{ep} in distinct tumor habitats

	LV-HC	LV-LC	HV-LC
ADC ($\times 10^{-3} mm^2/s$)	0.176	1.609	1.094
$K^{trans}(min^{-1})$	0.099	0.141	1.032
V_e	0.196	0.318	0.688
$K_{ep}(min^{-1})$	0.319	0.362	1.179

ADC = Apparent Diffusion Coefficient; K^{trans} = Volume Transfer Constant; V_e = extravascular extracellular volume fraction; K_{ep} = Flux Rate Constant

Table 4 Comparison of the volume proportion of tumor habitats between HER2-positive and HER2-negative breast cancer

	HER2-positive (*n* = 24)	HER2-negative (*n* = 52)	*p*-value
Proportion of LV-HC (%)	34.54(13.05 ~ 57.45)	56.95(32.96 ~ 78.60)	0.005[a]
Proportion of LV-LC (%)	37.89(18.64 ~ 54.58)	22.07(13.24 ~ 42.15)	0.049[a]
Proportion of HV-LC (%)	20.73(13.10 ~ 32.27)	13.76(2.40 ~ 25.41)	0.028[a]

[a] rank sum test

Table 5 Comparison of the volume proportion of tumor habitats between HER2-low and HER2-zero breast cancer

	HER-2 low (*n* = 33)	HER-2 zero (*n* = 19)	*p*-value
Proportion of LV-HC (%)	63.56(37.09 ~ 84.54)	54.65(25.51 ~ 72.92)	0.168[a]
Proportion of LV-LC (%)	17.59(4.56 ~ 37.27)	36.65(18.87 ~ 56.03)	0.014[a]
Proportion of HV-LC (%)	15.33(2.92 ~ 26.15)	6.07(0.26 ~ 25.00)	0.591[a]

[a] rank sum test

The clinical impact of intra-tumor heterogeneity

Breast cancer, as a highly heterogeneous tumor, has significant differences in its internal microenvironment, which greatly affects treatment outcomes [14, 16]. Intra-tumor heterogeneity is not only reflected in the variation of cell types and genetic mutations but also in differences in vascularity and cell proliferation across different tumor regions. Some areas within the tumor may experience insufficient angiogenesis, leading to hypoxic conditions that can impact tumor cell metabolism and therapeutic responses.

Furthermore, intra-tumor heterogeneity also complicates personalized treatment in breast cancer. Different sub-regions within the same tumor may exhibit varying responses to treatment. Even for the same patient, the tumor may react differently at different stages of treatment. For instance, some tumor regions may exhibit higher proliferation rates and angiogenesis, while other regions may show lower cell activity. These differences lead to varying sensitivities to drugs in different tumor areas, which, in turn, affects the overall treatment response. Therefore, understanding intra-tumor heterogeneity is crucial for developing more personalized treatment strategies.

Discovery of distinct tumor habitat and quantification of vascularity and cellularity heterogeneity in breast cancer

In this study, the FCM algorithm was used to conduct clustering analysis on the ADC, K^{trans}, V_e and K_{ep} maps, which facilitated breast cancer segmentation into three tumor habitats. According to the mean value of each quantitative index, the physiological significance of tumor habitats was evaluated, and it was divided into relatively LV-HC, relatively LV-LC, and relatively HV-LC. This proved to be helpful for the study of spatial heterogeneity of breast cancer.

Previously, AK Syed, JG Whisenant, SL Barnes, AG Sorace and TE Yankeelov [22] identified three tumor habitats in both triple-negative and HER2-positive breast cancer models by pathological histology, including high vascularity-high cellularity, low vascularity-high cellularity and low vascularity-low cellularity. A similar study was conducted by AS Kazerouni, DA Hormuth, 2nd, T Davis, MJ Bloom, S Mounho, G Rahman, J Virostko, TE Yankeelov and AG Sorace [23].

In another way, our study did not identify the tumor habitat characterized by high vascularity-high cellularity. Instead, it uncovered a previously unreported tumor habitat with relatively high vascularity-low cellularity. There are several potential reasons for these disparities. First, female with breast cancer were not grouped according to molecular subtypes in this study, whereas previous researches analyzed animal models of breast cancer with specific molecular subtypes. Second, there were difference in MRI scanners and scanning parameters.

Comparison of the volume percentage of tumor habitat with different HER-2 expression levels

In this study, we observed variations in the proportional volume of different tumor habitats within the breast cancers with varying HER2 expression levels. Specifically, we found that the proportional volume of the first tumor habitat was higher in the HER2-negative group compared to the HER2-positive group. This discrepancy could be attributed to the fact that the first tumor habitat exhibited relatively LV-HC. Previous preclinical studies have indicated that the baseline volume of the tumor habitat with physiological characteristics of LV-HC was higher in triple-negative breast cancer animal models compared to HER2-positive group [22]. Second, we observed that the proportional volume of the second and third tumor habitats was higher in the HER2-positive group compared to the HER2-negative group. The second tumor habitat was characterized by relatively LV-LC, while the third tumor habitat exhibited relatively HV-LC. The quantitative indicators representing vascularity, namely K^{trans} and K_{ep}, had mean values of 0.141 (min^{-1}) and 0.362 (min^{-1}) for the second tumor habitat, and exhibited mean values of 1.032 (min^{-1}) and 1.179 (min^{-1}) for the third tumor habitat. In contrast, the first tumor habitat exhibited mean values of 0.099 (min^{-1}) and 0.319 (min^{-1}) for K^{trans} and K_{ep}, respectively. These findings indicated higher levels of vascularity in the second and third tumor habitats compared to the first tumor habitat. This may be due to the involvement of HER2 in the expression of vascular endothelial growth factor and its association with tumor angiogenesis. Therefore, the relatively high vascularity levels of the second and third tumor habitats in the HER2-positive group were relatively higher. Finally, we also observed a higher proportional volume of the second tumor habitat in the HER2-zero group compared to the HER2-low group, which exhibited relatively low vascularity-low cellularity, possibly attributable to the lack of HER2 expression in the HER2-0 group.

The efficacy of neoadjuvant therapy in breast cancer is related to the proportional volume of tumor habitat

Neoadjuvant therapy is a crucial component in the current comprehensive treatment of breast cancer. This study found that the proportional volume of tumor habitat within breast cancer is related to the efficacy of neoadjuvant therapy. In this study, we found a negative correlation between the proportional volume of the first tumor habitat and the MP grading. The first tumor habitat is characterized by LV-HC, which may suggest that tumor cells in this region have adapted to a hypoxic and nutrient-poor microenvironment. This further has the potential to resist apoptosis and continue to proliferate [33]. Previous studies have shown that their metabolism becomes more active and stimulates tumor angiogenesis when tumor cells proliferate rapidly. However, the blood vessels generated at this time are abnormal and non-functional, making it easy for the tumor to require more oxygen than it receives. This leads to an increase in hypoxic regions within the tumor, which in turn leads to an increase in the tolerance of tumor cells to chemotherapy, radiation therapy and immunotherapy [16].

Previous preclinical study has found that multi-parameter MRI can be used to identify tumor habitats with different physiological states within breast cancer tumors and have been validated by pathological histology, including hypoxic habitats associated with treatment resistance [24]. In this study, we observed a negative correlation between the proportional volume of the first tumor habitat of breast cancer and the efficacy of neoadjuvant therapy. This negative correlation may be attributed to the fact that a lower proportion of hypoxic regions within the lesion indicates a lower proportion of drug-resistant areas in breast cancer, thus improving the efficacy of neoadjuvant therapy.

Comparison between MRI/HI and pathology

Pathology is widely considered the gold standard for assessing tumor heterogeneity, providing detailed histological features of tumor cells and molecular marker expression. The strength of pathology lies in its ability to provide high-precision, quantitative data on the histological characteristics of tumors. However, pathology also has limitations: it relies on tissue samples obtained via invasive procedures, often with limited sample size, and typically reflects only a small region of the tumor. This restricts its ability to comprehensively assess intratumor heterogeneity. Additionally, pathology analysis is subject to observer variability due to manual interpretation, which can affect diagnostic consistency.

In contrast to traditional pathology, MRI provides non-invasive, multi-dimensional, and multi-parametric information, including tumor anatomy, function, metabolism, and hemodynamics, with high soft tissue resolution. This allows MRI to offer a more comprehensive evaluation of tumor heterogeneity, especially in detecting tumors with unclear boundaries or small lesions. However, MRI has limitations, including the need for high-quality image acquisition and complex image analysis procedures, and some details of certain regions may be difficult to capture. HI, which integrates multi-parametric imaging techniques, further enhances tumor heterogeneity quantification by segmenting the tumor into different sub-regions through clustering analysis. HI's strength lies in providing a detailed and comprehensive quantitative description of tumor heterogeneity, offering valuable insights for personalized treatment. However, it also faces challenges, including high technical demands and reliance on advanced image processing and data analysis methods.

Explanations for the absence of the "high vascularity-high cellularity" habitat

Although prior preclinical studies have reported the presence of a high vascularity–high cellularity (HV-HC) habitat in breast cancer models, our clinical dataset did not identify this specific subregion. Instead, we identified three alternative physiologically plausible habitats, including a high vascularity–low cellularity (HV-LC) region and a low vascularity–high cellularity (LV-HC) region. In addition to potential differences between animal models and clinical human data, we propose a biological rationale for this observation.

Previous studies have shown that during periods of rapid tumor cell proliferation, angiogenesis is upregulated due to increased metabolic demand. However, the resulting neovasculature is often abnormal in structure and dysfunctional in perfusion. These vessels may lack efficient flow despite their increased density, leading to areas with high cellularity but relatively poor perfusion—manifesting as LV-HC rather than HV-HC regions. This paradoxical relationship between proliferation and perfusion may underlie the absence of the HV-HC habitat in our analysis.

Moreover, due to the current lack of standardized data on the expected frequency of HV-HC habitats in human breast cancer cohorts, we were unable to statistically validate this absence in comparison to previous studies. Future investigations with larger, subtype-stratified cohorts and pre/post-treatment imaging may help clarify whether HV-HC regions are specific to certain tumor phenotypes or confined to preclinical models.

Limitations and future works

There are some limitations to our study. First, our study was limited by a finite sample size. In the future, it is imperative to continuously augment the sample size. With a sufficient sample size, additional analysis can be performed on breast cancer patients sharing the same molecular subtypes, which can help investigate the inter-tumor heterogeneity within lesions of identical molecular subtypes. Second, our experiment did not incorporate data of diffusion kurtosis imaging (DKI), due to the limited availability of samples with DKI sequences. DKI can offer more precise and realistic insights into the microstructural properties of tissues, which enable a more accurate quantitative assessment of water molecule diffusion within and outside tumor cells. Therefore, it would be advantageous to include DKI data in future analyses when a sufficient sample size becomes accessible. Third, although our study utilized habitat imaging to divide the interior of breast cancer into sub-regions with different physiological significance, it lacked potential histopathological validation. In the future, we will attempt to interpret and validate the findings by matching the sub-regions of habitat depicted in MRI images with corresponding tissue sections. Fourth, this study did not include a direct comparative analysis of HI with these traditional biomarkers. Future research will include systematic comparisons between HI and biomarkers such as Ki-67, tumor grading, and conventional MRI metrics (e.g., K^{trans}, V_e) to evaluate the relative advantages and predictive capabilities of HI as a non-invasive imaging biomarker.

This study demonstrates the potential of Habitat Imaging (HI) for tumor characterization in breast cancer, particularly in predicting HER2 expression levels and assessing neoadjuvant therapy efficacy. However, despite the promising initial results, further validation and optimization are required. Future research should include the following key steps:

Prospective Clinical Trials: To validate the application of HI across different subtypes of breast cancer, we plan to conduct prospective clinical trials. By comparing HI

with existing clinical standards (such as histological subtypes, Ki-67 expression, etc.), we can further assess its clinical value.

Automated Segmentation Techniques: In future studies, we will introduce automated segmentation techniques, utilizing deep learning algorithms to improve segmentation efficiency and accuracy, further advancing the application of HI in large-scale clinical data.

Deep Learning Approaches: We also aim to integrate deep learning approaches to analyze patterns in HI data, with the goal of developing predictive models. This will help enhance HI's predictive capability in various clinical scenarios, such as its application in patients with varying levels of HER2 expression.

Summary

In summary, we first integrated DWI with DCE-MRI to comprehensively evaluate breast cancer heterogeneity from two physiological perspectives: cellular proliferation (via ADC and V_e) and vascular perfusion (via K^{trans} and K_{ep}), demonstrating a novel multi-dimensional and synergistic imaging approach. Second, we established a habitat imaging model based on multiparametric MRI and applied fuzzy clustering to segment tumors into subregions with distinct vascularity and cellularity profiles. This enabled a precise and quantitative assessment of both intra- and inter-tumoral heterogeneity, highlighting methodological and conceptual innovation. Finally, addressing the clinical challenge posed by the high heterogeneity of breast cancer that hampers personalized therapy, our study proposes a noninvasive and visual evaluation strategy. We demonstrated correlations between specific tumor habitats (e.g., LV-HC) and HER2 expression levels as well as neoadjuvant therapy response, underscoring the translational potential and clinical utility of this imaging approach.

Conclusion

Our study demonstrates that HI based on multi-parametric MRI can quantitatively visualize the heterogeneity of vascularity and cellularity within breast cancer lesions. There are differences in the proportional volume of various tumor habitats between breast cancer with different HER2 expression levels, which may be related to differences in vascularity and cellularity within the lesions due to different HER2 expression levels. There is a correlation between the proportional volume of tumor habitats within breast cancer lesions and the efficacy of neoadjuvant therapy, which may be related to the effect of blood flow perfusion and cell proliferation within the lesion on the patient's response to treatment. This suggests that HI may become a non-invasive imaging biomarker for predicting the efficacy of neoadjuvant therapy in breast cancer.

Supplementary Information

The online version contains supplementary material available at https://doi.org/10.1186/s12880-025-01698-x.

Supplementary Material 1

Acknowledgements

Not applicable.

Author contributions

X.-L.Z: Methodology, Software, Validation, Visualization, Writing – review & editing; X.-Y.C: Methodology, Formal analysis, Investigation, Visualization, Writing – original draft; Y.F: Formal analysis, Data curation; H.Z: Formal analysis, Investigation; Y.L: Conceptualization, Resources, Supervision, Funding acquisition, Project administration, Writing – review & editing.

Funding

This study was supported by the National Natural Science Foundation of China (82071973), Guangdong Basic and Applied Basic Research Foundation (2023A1515010326, 2020A1515011022) and Key Research Platform and Project of Guangdong University (2022ZDZX2020).

Data availability

The data and materials used for the analysis are available from the corresponding author upon request.

Declarations

Ethics approval and consent to participate

Institutional Review Board approval was obtained. This study was approved by the Ethics Committee of the Second Affiliated Hospital of Shantou University Medical College (2020-34), which waived the requirement for written informed consent owing to the use of de-identified retrospective data. The authors confirm that all experiments involving humans and/or the use of human tissue samples were performed in accordance with the Declaration of Helsinki.

Consent for publication

Not applicable.

Competing interests

The authors declare no competing interests.

Received: 13 January 2025 / Accepted: 28 April 2025
Published online: 13 May 2025

References

1. Sung H, Ferlay J, Siegel RL, Laversanne M, Soerjomataram I, Jemal A, Bray F. Global Cancer statistics 2020: GLOBOCAN estimates of incidence and mortality worldwide for 36 cancers in 185 countries. CA Cancer J Clin. 2021;71(3):209–49.
2. McDonald ES, Clark AS, Tchou J, Zhang P, Freedman GM. Clinical diagnosis and management of breast Cancer. J Nucl Med. 2016;57(Suppl 1):S9–16.
3. Pashayan N, Antoniou AC, Ivanus U, Esserman LJ, Easton DF, French D, Sroczynski G, Hall P, Cuzick J, Evans DG, et al. Personalized early detection and prevention of breast cancer: ENVISION consensus statement. Nat Rev Clin Oncol. 2020;17(11):687–705.
4. Bettaieb A, Paul C, Plenchette S, Shan J, Chouchane L, Ghiringhelli F. Precision medicine in breast cancer: reality or Utopia? J Transl Med. 2017;15(1):139.
5. Marusyk A, Polyak K. Tumor heterogeneity: causes and consequences. Biochim Biophys Acta. 2010;1805(1):105–17.
6. Koren S, Bentires-Alj M. Breast tumor heterogeneity: source of fitness, hurdle for therapy. Mol Cell. 2015;60(4):537–46.
7. Burstein HJ, Curigliano G, Thurlimann B, Weber WP, Poortmans P, Regan MM, Senn HJ, Winer EP, Gnant M. Panelists of the St Gallen consensus C: customizing local and systemic therapies for women with early breast cancer: the

St. Gallen international consensus guidelines for treatment of early breast cancer 2021. Ann Oncol. 2021;32(10):1216–35.
8. Marchio C, Annaratone L, Marques A, Casorzo L, Berrino E, Sapino A. Evolving concepts in HER2 evaluation in breast cancer: heterogeneity, HER2-low carcinomas and beyond. Semin Cancer Biol. 2021;72:123–35.
9. Wolff AC, Hammond MEH, Allison KH, Harvey BE, Mangu PB, Bartlett JMS, Bilous M, Ellis IO, Fitzgibbons P, Hanna W, et al. Human epidermal growth factor receptor 2 testing in breast cancer: American society of clinical oncology/college of American pathologists clinical practice guideline focused update. J Clin Oncol. 2018;36(20):2105–22.
10. Tarantino P, Viale G, Press MF, Hu X, Penault-Llorca F, Bardia A, Batistatou A, Burstein HJ, Carey LA, Cortes J, et al. ESMO expert consensus statements (ECS) on the definition, diagnosis, and management of HER2-low breast cancer. Ann Oncol. 2023;34(8):645–59.
11. Press MF, Lenz HJ. EGFR, HER2 and VEGF pathways: validated targets for cancer treatment. Drugs. 2007;67(14):2045–75.
12. Alameddine RS, Otrock ZK, Awada A, Shamseddine A. Crosstalk between HER2 signaling and angiogenesis in breast cancer. Curr Opin Oncol. 2013;25(3):313–24.
13. Modi S, Jacot W, Yamashita T, Sohn J, Vidal M, Tokunaga E, Tsurutani J, Ueno NT, Prat A, Chae YS, et al. Trastuzumab Deruxtecan in previously treated HER2-Low advanced breast Cancer. N Engl J Med. 2022;387(1):9–20.
14. Vitale I, Shema E, Loi S, Galluzzi L. Intratumoral heterogeneity in cancer progression and response to immunotherapy. Nat Med. 2021;27(2):212–24.
15. Swanton C. Intratumor heterogeneity: evolution through space and time. Cancer Res. 2012;72(19):4875–82.
16. Chen Z, Han F, Du Y, Shi H, Zhou W. Hypoxic microenvironment in cancer: molecular mechanisms and therapeutic interventions. Signal Transduct Target Ther. 2023;8(1):70.
17. Wang Y, Waters J, Leung ML, Unruh A, Roh W, Shi X, Chen K, Scheet P, Vattathil S, Liang H, et al. Clonal evolution in breast cancer revealed by single nucleus genome sequencing. Nature. 2014;512(7513):155–60.
18. Solanki M, Visscher D. Pathology of breast cancer in the last half century. Hum Pathol. 2020;95:137–48.
19. Leithner D, Wengert GJ, Helbich TH, Thakur S, Ochoa-Albiztegui RE, Morris EA, Pinker K. Clinical role of breast MRI now and going forward. Clin Radiol. 2018;73(8):700–14.
20. Huang Y, Lin Y, Hu W, Ma C, Lin W, Wang Z, Liang J, Ye W, Zhao J, Wu R. Diffusion kurtosis at 3.0T as an in vivo imaging marker for breast Cancer characterization: correlation with prognostic factors. J Magn Reson Imaging. 2019;49(3):845–56.
21. Wu J, Cao G, Sun X, Lee J, Rubin DL, Napel S, Kurian AW, Daniel BL, Li R. Intratumoral Spatial heterogeneity at perfusion MR imaging predicts Recurrence-free survival in locally advanced breast Cancer treated with neoadjuvant chemotherapy. Radiology. 2018;288(1):26–35.
22. Syed AK, Whisenant JG, Barnes SL, Sorace AG, Yankeelov TE. Multiparametric analysis of longitudinal quantitative MRI data to identify distinct tumor habitats in preclinical models of breast Cancer. Cancers 2020:12(6).
23. Kazerouni AS, Hormuth DA 2nd, Davis T, Bloom MJ, Mounho S, Rahman G, Virostko J, Yankeelov TE, Sorace AG. Quantifying tumor heterogeneity via MRI habitats to characterize microenvironmental alterations in HER2 + Breast Cancer. Cancers (Basel) 2022:14(7).
24. Jardim-Perassi BV, Huang S, Dominguez-Viqueira W, Poleszczuk J, Budzevich MM, Abdalah MA, Pillai SR, Ruiz E, Bui MM, Zuccari D, et al. Multiparametric MRI and coregistered histology identify tumor habitats in breast Cancer mouse models. Cancer Res. 2019;79(15):3952–64.
25. Mohamed N, Ahmed SMY, Nevin Mohamed AA, Farag T, Moriarty. A modified fuzzy C-means algorithm for bias field Estimation and segmentation of MRI data. IEEE Trans Med Imaging. 2002;21(3):193–9.
26. Zhang X, Pan W, Wu Z, Chen J, Mao Y, Wu R. Robust image segmentation using fuzzy c-means clustering with Spatial information based on total generalized variation. IEEE Access. 2020;8:95681–97.
27. Xue Y, Feng R, Cui S, Yu B. Traffic status evolution trend prediction based on congestion propagation effects under rainy weather. J Adv Transp. 2020;2020(1):8850123.
28. Rathika S, Mahendran K, Sudarsan H, Ananth SV. Novel neural network classification of maternal fetal ultrasound planes through optimized feature selection. BMC Med Imaging. 2024;24(1):337.
29. Ogston KN, Miller ID, Payne S, Hutcheon AW, Sarkar TK, Smith I, Schofield A, Heys SD. A new histological grading system to assess response of breast cancers to primary chemotherapy: prognostic significance and survival. Breast. 2003;12(5):320–7.
30. Wang X, Hu W. MRCT and CT in the diagnosis of pediatric disease imaging: assessing imaging performance and clinical effects. BMC Med Imaging. 2024;24(1):96.
31. Xie W, Cao L, Yu J, Tian A, Wang J, Lin R. (18)F-FDG PET/CT metabolic parameter changes to assess vascular inflammatory response in patients with diffuse large B-cell lymphoma. BMC Med Imaging. 2025;25(1):81.
32. Harbeck N, Penault-Llorca F, Cortes J, Gnant M, Houssami N, Poortmans P, Ruddy K, Tsang J, Cardoso F. Breast cancer. Nat Rev Dis Primers. 2019;5(1):66.
33. Gatenby RA, Grove O, Gillies RJ. Quantitative imaging in cancer evolution and ecology. Radiology. 2013;269(1):8–15.

Publisher's note